PHYSICAL REVIEW B VOLUME 35, NUMBER 3 15 JANUARY 1987-II

Generalized Ramsauer-Townsend resonance in angle-resolved photoemission extended fine-structure oscillations

J. J. Barton, Z. Hussain,* and D. A. Shirley
Materials and Molecular Research Division, Lawrence Berkeley Laboratory, University of California, Berkeley, California 94720 and Department of Chemistry, University of California, Berkeley, California 94720
(Received 16 April 1986)

We observe a resonance in the scattering amplitude for S(1s) photoelectrons from Ni atoms and interpret this resonance as a dip in the Ni atom partial cross section for electron scattering related to the Ramsauer-Townsend effect. This generalized Ramsauer-Townsend effect occurs at a particular energy and angle rather than in the total elastic cross section. We show that the resonance energy is sensitive to curved-wave corrections and, after including multiple-scattering effects, we derive the S—Ni bond length in $c(2\times2)$S/Ni(100) from the angle-resolved photoemission extended fine-structure oscillations arising from the scattering of S(1s) photoelectrons off of nearest-neighbor Ni atoms in the presence of the generalized Ramsauer-Townsend resonance. We find this bond length to be 2.20±0.03 Å corresponding to a S-Ni interplanar distance ($d_\perp$) of 1.32±0.04 Å.

I. INTRODUCTION

The nature of the core-level photoemission intensity oscillations known as photoelectron diffraction has been substantially clarified by new theoretical[1,2] and experimental work which shows that these oscillations—caused by interference between direct and scattered photoemission probability amplitude[3,4]— are qualitatively predicted by scattering path-length differences. A complete understanding of the physics of these oscillations has important consequences for the use of photoelectron diffraction as a technique for determining surface structure: The total scattering path-length difference is the sum of a geometrical path length and an ion-core potential phase-shift function of the scattering atom, allowing the geometry to be deduced if the potential can be adequately modeled. While most of the energy-dependent photoelectron diffraction measurements[5,6] have been made in the kinetic-energy range from 20 to 150 eV, we have recently[7,8] been concentrating on photoelectron energies between 100 and 600 eV. These intermediate energies and the wider energy range are advantageous if we wish to concentrate on structure determination because the potential phase-shift functions are less sensitive to chemical effects, the photoabsorption cross section has less structure, and the photoelectron scattering partial cross section is more anisotropic giving a simpler and more structure-sensitive spectrum. For very similar reasons x-ray-absorption fine-structure spectroscopies have been divided into x-ray-absorption near-edge structure (XANES or NEXAFS) at low energies and extended x-ray-absorption fine structure (EXAFS) in the intermediate 100—1000 eV range. We refer to the core-level angle-resolved photoemission measurements in the 100—1000 eV intermediate energy range as angle-resolved photoemission extended fine structure (ARPEFS).

To concentrate on the oscillating, nonatomic signal we remove the slowly varying part I_0, of the intensity I, to form $\chi=(I-I_0)/I_0$. Every model for ARPEFS predicts that the oscillations, expressed as a function of electron wave number k are cosinusoidal,

$$\chi(k)=\sum_j A_j(k)\cos[kr_j(1-\cos\theta_j)+\phi_j(k)] ,$$

where $A_j(k)$ is an amplitude function, ϕ_j is a scattering potential phase function, and $(r_j-r_j\cos\theta_j)$ is the geometrical path-length difference for bond length r_j and scattering angle θ_j. The sum on j extends over all atoms near the photoemitter which have significant amplitude. In the simplest case, the amplitude function is large for only a few atoms and has little structure as a function of k, and the phase similarly benign. Then the ARPEFS curve may be Fourier analyzed and—provided Fourier resolution is adequate—the Fourier amplitude spectrum should have peaks corresponding to scattering path-length differences.[7] If, on the other hand, the amplitude function is not a smooth envelope, the Fourier spectrum for the corresponding scattering event will not peak at the scattering path-length difference. In this paper we investigate structure determination with ARPEFS in the case that the scattering potential for nearest-neighbor scattering atom has a strong amplitude dependence caused by an interesting resonance related to the Ramsauer-Townsend effect.

We have selected $c(2\times2)$S/Ni(100) for our study primarily because the S adsorption site and the S—Ni bond length have been reported previously and the overlayer can be reproduced easily. Elsewhere we report[9] a study of the S (1s) ARPEFS from $c(2\times2)$S/Ni(100), concentrating on the scattering events which have Fourier peaks near the scattering path-length difference. Here we will discuss normal emission S(1s) ARPEFS from the nearest-neighbor Ni atoms in the fourfold hollow site. The amplitude for the scattering of S photoelectrons from Ni potentials into the normal direction dips sharply as the energy is scanned leading to a split Fourier peak.

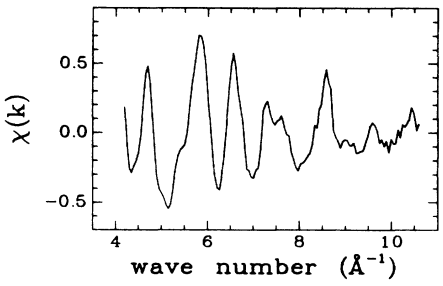

FIG. 1. S(1s) ARPEFS oscillations from $c(2\times2)$S/Ni(001) along normal emission ([001]). The experimental kinetic-energy scale has been converted to a wave-number scale using an inner potential of 10.5 eV, and the resulting curve has been interpolated with a numerical spline to an even mesh of 128 points.

II. EXPERIMENTAL

We have given a thorough discussion of our measurement procedure in Ref. 9 so we will be brief here. Our sample was prepared in a standard fashion: a mirror-finish, oriented Ni(001) single crystal was cleaned in vacuum, exposed to H_2S(g), and heated briefly to 200°C to give a very sharp $c(2\times2)$S/Ni(100) LEED pattern. This sample was illuminated by soft x rays from the Stanford Synchrotron Radiation Laboratory Jumbo monochromator[10] and S(1s) angle-resolved photoemission intensity spectra were measured every 3 eV for photon energies between 2532 and 2950 eV. Assuming that the x rays are completely polarized in the plane of the synchrotron storage ring, we oriented the Ni crystal to place the electric vector of the light $\hat{\epsilon}$, 30° from the surface normal toward a [110] direction and rotated the angle-resolved electron energy analyzer to collect spectra along the surface normal. The individual photoemission measurements were reduced to partial cross-section measurements in the fashion described in Ref. 9.

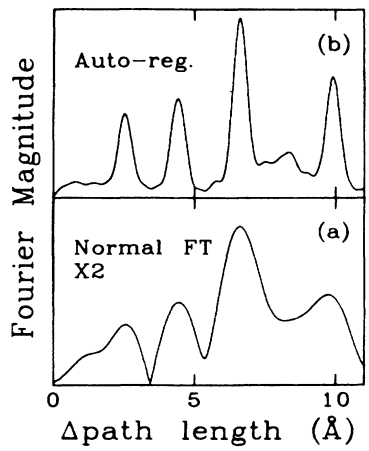

FIG. 2. Fourier transform magnitudes vs scattering path-length difference for k times the data in Fig. 1. In the lower panel (a), the conventional Fourier transform was applied; the upper panel (b) was obtained with the autoregressive linear prediction method described in Ref. 11.

The resulting ARPEFS curve $\chi(k)$ is given in Fig. 1. The energy scale has been converted to a wave-number scale using an inner potential of +10.5 eV. The curve is seen to be dominated by an oscillation with ~6 cycles in 2π Å^{-1}, corresponding to an interference path length of 6 Å. Since we know the nearest-neighbor bond length in this system is ~2.2 Å corresponding to a maximum path-length difference of 4.4 Å, we can conclude that the nearest-neighbor scattering does not dominate this curve.

Fourier transforms of this curve are shown in Fig. 2. For the lower panel, Fig. 2(a), we have multiplied $k\chi(k)$ by a Gaussian of full width at half maximum of 4 Å^{-1} centered on the data range, added zeros to fill 2048 cells, and applied the fast Fourier transform; the Fourier transform magnitude is plotted versus path-length difference. In the upper panel the autoregressive Fourier method described in Ref. 11 has been applied to $k\chi(k)$ and the resulting extrapolated sequence has been multiplied by a Gaussian of 12 Å^{-1} full width at half maximum.

The peaks in the Fourier spectrum above 5-Å path-length difference have been discussed in Ref. 9. The path-length difference derived from the positions of these Fourier peaks is approximately equal to the scattering path-length difference for backscattering Ni atoms in the second and third Ni layers. The positions of the two peaks below 5 Å do not correspond to any path-length difference, and no feature in the Fourier spectrum appears near 3.5 Å where we would expect a scattering path-length due to Ni nearest neighbors (assuming a fourfold hollow adsorption and reasonable S—Ni bond distances). The physical origin of these peaks is the subject of this paper.

III. GENERALIZED RAMSAUER-TOWNSEND RESONANCE

The lack of correspondence between the scattering path-length difference for nearest-neighbor Ni atoms and Fourier spectrum peaks is caused by a strong dip in the scattering power for Ni as a function of energy which occurs for scattering angles near those appropriate for normal emission from $c(2\times2)$S/Ni(001). This dip is related to the well-known Ramsauer-Townsend electron scattering resonance,[12] and hence we call this amplitude effect a generalized Ramsauer-Townsend (GRT) resonance.

Ramsauer and Townsend observed that argon becomes transparent to electrons at 0.7 eV. The origin of this surprising lack of scattering, suggested by N. Böhr and verified by Faxen and Holtsmark,[12] follows from the partial-wave formula for the (complex) scattering amplitude for electrons,

$$f(\theta,k)=\frac{1}{2ik}\sum_{l=0}^{\infty}(2l+1)P_l(\cos\theta)(e^{2i\delta_l}-1)\ ,$$

where $\delta_l(k)$ are the ion-core partial-wave phase shifts. At very low kinetic energies only δ_0, the isotropic s wave, contributes to the scattered wave. If, as is the case for Ar

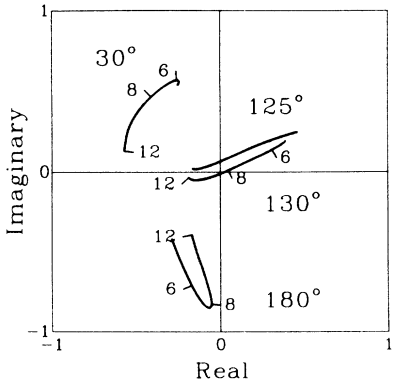

FIG. 3. Ni scattering amplitudes calculated in the plane-wave limit. Each solid line represents the scattering amplitude for the scattering angle indicated. For each scattering angle the amplitude was calculated for wave numbers from 5–12 Å^{-1}; the labeled tick marks give some indication of the wave-number scale. The amplitudes are plotted in the complex plane to illustrate the connection between scattering intensity and phase shift. Note that the scattering intensity is nearly zero for $\theta_j = 130°$ and $k = 8$ Å^{-1}.

at 0.7 eV, the value of the s phase shift was exactly 180°, then even this term goes to zero and the amplitude $f(\theta,k)$ becomes very small for all angles.

Our generalized Ramsauer-Townsend effect is more complicated.[13] At higher energies many partial waves contribute to the scattering amplitude. Then only with the proper linear combination of angular factors $(2l+1)$ $P_l(\cos\theta)$, and energy factors $(e^{2i\delta_l}-1)$, will the scattering amplitude be zero. Thus while the classical Ramsauer-Townsend effect gives zero amplitude at all angles and very low energy based on special behavior by one phase shift, our generalized Ramsauer-Townsend effect occurs at special angles and energies with many phase shifts involved.

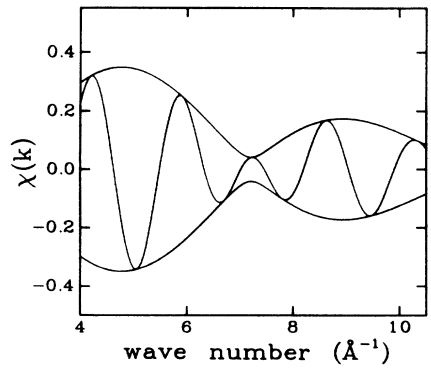

FIG. 4. Fourier filtered ARPEFS data. The Fourier spectrum from Fig. 2 was zeroed above 5.1 Å and backtransformed, the amplitude envelope is also plotted as obtained from the complex backtransformation.

Some ideas about the consequences of this effect can be derived from Fig. 3. Scattering amplitudes for four different angles are plotted in the complex plane. For each angle a line represents $f(k,\theta_j)$ for $k = 4$ Å^{-1} (60 eV) to $k = 12$ Å^{-1} (550 eV). The distance from the origin to a point on the line represents the scattering power for that angle and energy; the angle from the positive real axis to that point gives the wave phase shift caused by the potential.

For $\theta_j = 180°$ we see the scattering power peaks broadly around $k = 6$ Å^{-1}. From $k = 4$ Å^{-1} the phase angle sweeps gently through $\sim 60°$. For $\theta_j = 130°$, however, the behavior is radically different. Now the scattering amplitude approaches the origin for $k = 8$ Å^{-1}. The amplitude falls nearly to zero here, and the phase angle sweeps rapidly through 180°. The behavior for $\theta_j = 125°$ is similar, but the phase angle is rotating in the opposite direction.

Clear evidence that the generalized Ramsauer-Townsend effect is responsible for splitting the Fourier peak expected near 3.5 Å into the two peaks actually observed in the Fourier spectrum is obtained by backtransforming just those Fourier coefficients whose frequencies are less than 5 Å. As shown in Fig. 4, the resulting filtered ARPEFS curve shows a beat pattern consistent with a 3.5-Å oscillation with a superimposed amplitude envelope which dips at $k = 7.5$ Å^{-1} If the phase-shift function is extracted from the filtered data,[14] it exhibits the phase jump of π characteristic of the GRT zero crossing as shown in Fig. 5.

In our initial attempts to use the Ni GRT resonance,[15] we sought to compare the observed phase jump to calculated Ni atom phase-shift functions. As is evident from a comparison of the experimental phase function to the theoretical phase function calculated in the plane-wave

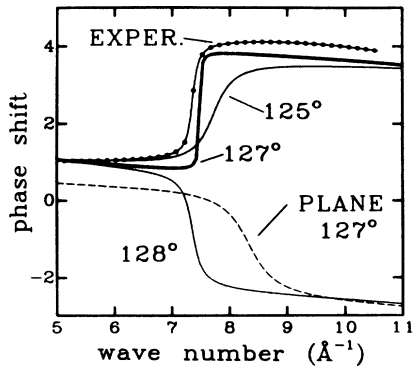

FIG. 5. Phase shifts for scattering from Ni. The dashed line shows the phase shift calculated with plane-wave theory $\theta_j = 127°$. The dotted line is the phase shift from the experimental curve shown in Fig. 2, where the first two Fourier peaks are backtransformed together. A factor of π for the sign difference between direct and scattered waves caused by the p-wave angular distribution has been added to the experimental phase and a nominal 3.5-Å path-length difference has been removed. The zero crossing jump in phase occurs too high in wave number for the plane-wave calculation. Solid lines are curved-wave calculations of the phase shift for the indicated scattering angles.

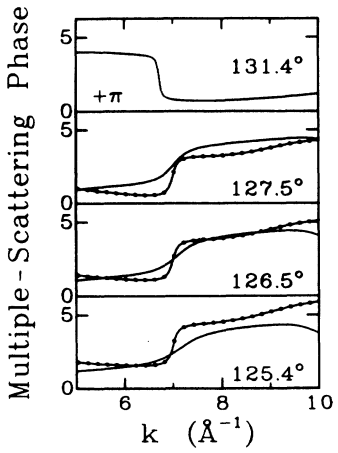

FIG. 6. Multiple-scattering GRT phase jumps. Each panel is labeled by the scattering angle for the Ni nearest neighbors. The dashed lines are phase jumps from the scattering calculation described in the text. The solid lines with circles are experimental phase jumps with geometrical path lengths removed. A phase equal to $3.57k$ radians was subtracted from both theory and experiment phase functions for comparing the $127.5°$ ($d_\perp = 1.35$ Å) phases, $3.49k$ radians from $126.5°$ ($d_\perp = 1.30$ Å), and $3.41k$ radians from $125.4°$ ($d_\perp = 1.25$ Å). As in Fig. 5, a factor of π for (-1) was added to all phase functions; an additional factor of π was added to the $131.4°$ phase for the purpose of display.

approximation (see Fig. 5, long-dashed curve), the resonance position in energy and angle is not correctly placed in this simple model. We therefore introduced curved wave front corrections[16] which, as the remaining curves in Fig. 5 demonstrate, places the calculated resonance of the experimentally observed energy. The fact that the resonance is sensitive to the wave-function calculation is not surprising given that several large partial-wave amplitudes must sum to zero at resonance: Any slight error in the weighting of these waves will shift the resonance position.

It would appear from Fig. 5 that we may assign the S—Ni bond length by comparing the observed phase-shift function shape to calculated functions which include the curved-wave corrections. The strong dependence of the GRT resonance on scattering angle would set a firm limit on the bond distance, and we would have an elegant method to estimate the surface bond angle.[8] However, this does not allow for the possibility of multiple scattering, and in view of the sensitivity of the resonance we must include this effect.

Fortunately, the calculation we require is very modest: We need only 20 scattering paths. The first four are the single scattering paths from the four Ni nearest the photoemitting S, with path lengths near 3.5 Å. The single scattering wave from the nearest neighbors can double scatter from either of two atoms in the S layer, giving a total of eight more paths near 4.4 Å. We also include scattering from four S atoms at 3.52 Å and four more at 4.98 Å even though the signal from these atoms is very small. Indeed, without curved-wave corrections[16] these S atoms would cancel in pairs: The phase of the direct wave incident upon one member of the pair is opposite the phase for the other. Of the 20 paths possible, only 10 are unique, and by employing the method of Ref. 2, the calculation requires no more effort than other steps in the data analysis process.

The resulting multiple-scattering phase functions are shown in Fig. 6. The multiple-scattering effect is small, but it is adding to a near zero signal. We find that the GRT resonance has been pushed up in angle from 127.5° in single scattering to 131° in multiple scattering. Figure 6 shows that the phase jump for 131.4° is on the opposite of the origin from the experimental jump, setting an upper bound on the S-Ni interlayer spacing, $d_\perp$ of 1.50 Å corresponding to 130.4°. Although this bound is not very useful, we can limit the value of $d_\perp$ much more closely by comparing the experimental phase functions to the multiple-scattering phase functions in Fig. 6. In each comparison, the same geometrical path-integral difference has been subtracted from both theory and experiment. The closest match is clearly for 126.5° corresponding to $d_\perp = 1.30$ Å. Because the angles 125.4° and 127.5° correspond, respectively, to $d_\perp = 1.25$ and $d_\perp = 1.35$ Å, this comparison alone has the precision to set small error limits on $d_\perp$ (perhaps $\pm 0.02 - 0.03$ Å).

We can also arrive at this conclusion by comparing the ARPEFS oscillations directly. Figure 7 compares the filtered experimental data to theory curves for S—Ni bond lengths of 2.16 ($d_\perp = 1.25$ Å), 2.19 ($d_\perp = 1.30$ Å), and 2.22 Å ($d_\perp = 1.35$ Å). Visual comparison is sufficient to exclude the two extreme geometries. Using the residual, an unweighted sum of the squared differences between experiment and theory, as a measure of the errors, we find a curve of error versus bond length whose minimum lies at 2.20 Å ($d_\perp = 1.32$ Å) as shown in Fig. 8. The theoretical

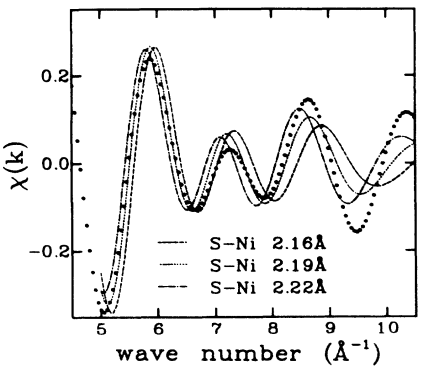

FIG. 7. Numerical simulation of the normal emission $S(1s)$ ARPEFS from $c(2\times2)$S/Ni(001) compared to Fourier filtered experimental data. The theory curves were calculated for all scattering paths less than 5.1 Å; the experimental Fourier transform in Fig. 2 was zeroed for frequencies above 5.1 Å and backtransformed to give the solid circles. Over the entire energy range, the frequency of the oscillations clearly matches the theory curve for a S—Ni bond length of 2.19 Å better than the curves for shorter or longer bond lengths.

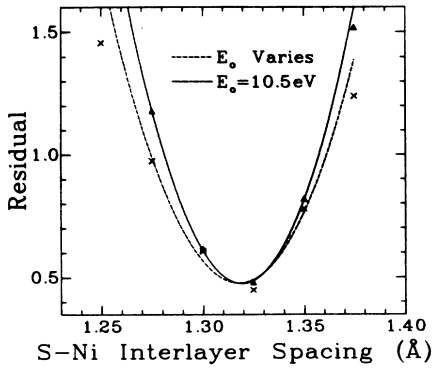

FIG. 8. Geometry search for S-Ni interlayer spacing. Plotted symbols are residuals from the least-squares fit of the numerical simulation curves to the Fourier filtered data. The residual is the unweighted sum of the squared differences between theory and experiment between 100 and 414 eV. The solid triangles give the residual for a fixed theory inner potential of 10.5 eV; the crosses correspond to fits in which the theory inner potential was varied. The solid curve is a parabolic fit to the four triangle points between 1.275 and 1.35 Å; the dashed curve is a parabolic fit to the four crosses in the same region.

curves were first scaled to the experiment to minimize their residual before constructing the curve of errors to reduce the influence of amplitude factors.

This preference for 2.20-Å bond length is not dependent on the inner potential: The same geometry is found even if both theory and experiment are placed on the experimental energy scale and the inner potential of the theory is allowed to vary. The curve of errors is less sensitive to the structure in this case as can be seen in Fig. 8 because the shift in E_0 partly compensates for an incorrect geometry. At the minimum residual, we find an inner potential of $+11$ eV, in good agreement with our original selection of $+10.5$ eV.

IV. DISCUSSION

Our measurement gives 2.20 Å for the S—Ni bond length in $c(2\times2)$S/Ni(001), in good agreement with previous studies.[9] In estimating the precision of our determination we note that the structure information is carried in medium frequency oscillations superimposed upon a smoothly varying signal, and that we have sampled this signal at a much higher frequency than is relevant for the structure analysis. Furthermore we have measured the oscillations over a wide enough energy range to ensure that errors in our reduction of the photoemission measurements to oscillations are minimal. The normal emission geometry is technically simpler to align, and any small angular errors in the emission direction are self-canceling in the sense that among the four nearest-neighbor Ni atoms every scattering path which lengthens with angle has a mate which shortens. We have varied the shape of the I_0 estimate by altering the stiffness of the numerical spline used to derive I_0 from the data without altering the back-transformed oscillations; the autoregressive Fourier transform is not essential for our analysis and the same results may be derived with conventional Fourier methods. A more complete discussion of possible errors may be found in Ref. 9. We believe our experimental precision is less than ±0.02 Å.

The accuracy of our bond length is unfortunately not entirely determined by experiment. Even though the Fourier filtering approach we have used here sufficiently restricts the theory problem so that we need not be concerned about convergence in multiple-scattering order or curved-wave corrections, our result still relies on accurate theoretical curves. By concentrating primarily on the frequency of the oscillations, our bond length is not sensitive to amplitude factors like inelastic mean free path, thermal averaging, or aperture integration. Furthermore, since the contribution of the path-length difference to the frequency is 20 times larger than the Ni potential phase shift and multiple-scattering corrections, even moderate errors in the theoretical contributions to the frequency will not disturb the bond length analysis. More serious sources of error in our procedure are the constant part of the multiple scattering phase shift function and the inner potential E_0. Either of these parameters will lead to geometry errors as the phase offset of theory and experiment is partial compensated by an erroneous shift in the theory path-length difference. Both the comparison of the curves in Fig. 7 and our residual analysis with variable E_0 in Fig. 8 argue that we have made no large error due to constant phase shift or inner potential here. Altogether we estimate our accuracy as ±0.02 Å in bond length or ±0.03 Å in the S-Ni interplaner spacing.

The theory errors are likely to be systematic, but we nevertheless quote our structure as S—Ni bond length of 2.20 ± 0.03 Å ($d_\perp=1.32\pm0.04$ Å). With additional study of the scattering potential for Ni and S, including the photoion-core potential, and additional measurements to ensure experimental reproducibility, the accuracy of this type of structure measurement should improve by about a factor of 2. We strongly emphasize that accurate structure work with extended fine structure requires a wide energy range. A short energy range is subject to error from construction of the $\chi(k)$ curve to Fourier analysis to theory comparison: The additional data points in an extended range set the trends of the low frequencies, and hence they provide more than a simple statistical improvement in our experiment.

Sagurton, Bullock, and Fadley have recently[17] studied the GRT resonance using single scattering theory, and they have concluded that the split Fourier peaks characteristic of the GRT resonance cannot be used for quantitative structural analyses. We believe that our work here demonstrates that this is not true, and rather than a serious liability, the GRT resonance has some interesting properties of its own. A more difficult problem is the contribution of double scattering to the frequency range occupied by the resonance, scattering which was omitted in the study of Sagurton *et al.* We have shown here that this problem can be overcome by applying the method of Ref. 2.

Our goal in this study has been to study the surface geometry and the generalized Ramsauer-Townsend resonance ultimately plays only a small role in our work. Understanding the GRT resonance is of course essential, but the presence of the resonance is a hindrance in the sense that the phase jump on resonance is sensitive to nonstructural parameters. A minor benefit of the resonance is the relatively flat (k-independent) nature of the Ni phase function above and below the resonance with a consequent negligible contribution to the oscillation frequency. We might imagine that the resonance itself could contribute to either the structure study in other surface systems or the study of surfaces in other ways. For example, first row adsorbates would scatter so little that direct comparison of the experimental phase function with the theory phase functions for various scattering angle might be sufficient to extract the structure. More intriguing, it may be possible to probe the electronic structure of the first layer of metal atoms in an adsorbate system by using the strong spin polarization[18] which accompanies the GRT. This polarization has its origin in the sensitivity of the resonance: If the scattering potential has any dependence on spin, then the resonance energy will be spin dependent. At a photoelectron energy and scattering angle which corresponds to the GRT resonance, the photoemission intensity will be sensitive to the spin state of the scattering atom.

V. CONCLUSION

We have observed a resonance in the scattering amplitude for S($1s$) photoelectrons from Ni atoms and interpreted this resonance as a dip in the Ni atom partial cross section for electron scattering related to the Ramsauer-Townsend effect. This generalized Ramsauer-Townsend effect occurs at a particular energy and angle rather than in the total elastic cross section. We have shown that the resonance energy is sensitive to curved-wave corrections and, after including some multiple-scattering effects, we have derived the S—Ni bond length of $c(2\times2)$S/Ni(100) from the ARPEFS oscillations from nearest-neighbor Ni atoms in the presence of the generalized Ramsauer-Townsend resonance. We find this bond length to be 2.20 $\pm$0.03 Å corresponding to a S-Ni interplanar distance ($d_\perp$) of 1.32$\pm$0.04 Å.

ACKNOWLEDGMENTS

This work was supported by the Director, Office of Energy Research, Office of Basic Energy Sciences, Chemical Sciences Division of the U. S. Department of Energy under Contract No. DE-AC03-76SF00098. It was performed at the Stanford Synchrotron Radiation Laboratory, which is supported by the U. S. Department of Energy's Office of Basic Energy Sciences.

---

*Permanent address: Department of Physics, University of Petroleum & Minerals, Dhahran 31261, Saudi Arabia.

[1]P. J. Orders and C. S. Fadley, Phys. Rev. B **27**, 781 (1983).

[2]J. J. Barton, S. W. Robey, and D. A. Shirley, Phys. Rev. B **34**, 778 (1986).

[3]A. Liebsch, Phys. Rev. Lett. **32**, 1203 (1974).

[4]P. A. Lee, Phys. Rev. B **13**, 5261 (1976).

[5]D. A. Shirley, C. R. Solid State Mater. Sci. **10**, 373 (1982).

[6]S. Y. Tong and C. H. Li, in *Chemistry and Physics of Solid Surface,* edited by R. Vanselow and W. England (CRC Press, Cleveland, 1982), Vol. III, p. 287.

[7]J. J. Barton, C. C. Bahr, Z. Hussain, S. W. Robey, J. G. Tobin, L. E. Klebanoff, and D. A. Shirley, Phys. Rev. Lett. **51**, 272 (1983).

[8]J. J. Barton, S. W. Robey, C. C. Bahr, and D. A. Shirley, in *The Structure of Surfaces,* Proceedings of the First International Conference, Berkeley, California, Vol. 2 of *Springer Series in Chemical Physics,* edited by M. A. Van Hove and S. Y. Tong (Springer, Berlin, 1985), p. 191.

[9]J. J. Barton, C. C. Bahr, S. W. Robey, Z. Hussain, E. Umbach, and D. A. Shirley, Phys. Rev. B **34**, 3807 (1986), and references therein.

[10]Z. Hussain, E. Umbach, D. A. Shirley, J. Stöhr, and J. Feldhaus, Nucl. Instrum. Methods **195**, 115 (1982).

[11]J. J. Barton and D. A. Shirley, Lawrence Berkeley Laboratory Report No. LBL-14758 (unpublished).

[12]H. Faxen and J. Holtsmark, Z. Phys. **45**, 307 (1927).

[13]For some elements the generalized Ramsauer-Townsend effect occurs between 3 and 12 Å at 180°. It then appears in the EXAFS spectrum. B. K. Teo and P. A. Lee, J. Am. Chem. Soc. **101**, 2815 (1979).

[14]G. Martens, P. Rabe, N. Schwentner, and A. Werner, Phys. Rev. B **17**, 1481 (1978).

[15]J. J. Barton, C. C. Bahr, Z. Hussain, S. W. Robey, L. E. Klebanoff, and D. A. Shirley, in *Science with Soft X Rays,* Vol. 447 of the *Proceedings of the Society of Photooptical Instrument Engineers,* edited by F. J. Himpsel and R. W. Klaffky (SPIE, Billingham, WA, 1984), p. 82.

[16]J. J. Barton and D. A. Shirley, Phys. Rev. B **32**, 1892 (1985).

[17]M. Sagurton, E. L. Bullock, and C. S. Fadley, Phys. Rev. B **30**, 7332 (1984).

[18]H. S. W. Massey, E. H. S. Burhop, and H. B. Gilbody, *Electronic and Ionic Impact Phenomena,* 2nd ed. (Oxford University, London, 1969), Vol. 1.